Energy distribution of H^- from the collision-induced three-particle breakup of H_3^+

O. Yenen, D. H. Jaecks, and L. M. Wiese
Behlen Laboratory of Physics, University of Nebraska, Lincoln, Nebraska 68588-0111
(Received 6 July 1988)

We have measured the laboratory energy distribution of H^- produced by the collision-induced dissociation of H_3^+ from He targets for incoming beam energies ranging from 2.417 to 7.0 keV. An approximate projectile frame energy distribution of H^- is also obtained. The most probable H^- projectile frame energy is estimated to be approximately 0.75 eV. We have also determined, from the shift in the position of the H^- laboratory peaks, an inelastic energy loss of 60 ± 12 eV for the excited H_3^+ ions producing near zero kinetic energies of H^- in the projectile frame. Our results suggest that H^- is produced by the electronic excitation of H_3^+ with subsequent dissociation into $H^+ + H^+ + H^-$. In this case the motion of the two H^+ ions is highly correlated. For the most probable c.m. energy of H^-, we put a lower limit of 163° on the correlation angle between the protons in the c.m. of dissociating H_3^+.

I. INTRODUCTION

From elementary particles to atomic physics, most of our understanding of nature is based on either two-body theories, where the system is reduced to the equivalent one-body problem, or statistical mechanics, where the average behavior of a large number of particles is described. In the latter case, the more particles participating in the process, the more kinematical aspects dominate the behavior of the system. This situation culminates in classical thermodynamics, where the dynamical aspect of the system manifests itself only in determining certain constants of the phenomenological laws obtained from the phase-space considerations, i.e., the kinematics of the process. Only when a small number of particles is observed do the dynamical aspects become important enough to alter the form of the laws instead of the values of the parameters. In the observation of natural phenomena, there are many instances where the number of interacting particles is larger than 2, but not large enough to allow a statistical treatment of the problem. The so-called "few-body" problem can be found in almost every branch of physics and its fundamental nature presents a challenge to all disciplines of physics.

Obviously, the simplest "few-body" system to study is the one formed by three interacting particles. In atomic and molecular physics, progress has been made in the analysis of the three-particle systems where the interaction is known to be the Coulomb interaction. The threshold behavior of electron-impact ionization cross sections has been a good example of the above-mentioned problem, where the incident electron, the emitted electron, and the remaining ion form a highly correlated Coulomb-interacting–three-body system, and has been subjected to numerous theoretical and experimental studies.[1]

Recently, the theory was extended to the fragmentation of three-body systems of arbitrary mass by Klar[2] for zero total angular momentum L, and by Feagin[3] for all values of L. Experimentally, one of the simplest systems to be compared with these theories is the near-threshold fragmentation of H_3^+ into the $H^+ + H^+ + H^-$ channel. The initial measurements of the laboratory angular distribution of H^- by Montgomery and Jaecks[4] proved that it is possible to produce large amounts of H^- from the dissociation of H_3^+ colliding at low-keV energies with He targets. The absolute total cross sections for this process are obtained by Alvarez *et al.*[5] by numerical integration of the laboratory differential H^- production cross sections. Montgomery and Jaecks[4] assumed that H^- is produced by the dissociation of an excited H_3^+ state into $H^+ + H^+ + H^-$. Their analysis of the laboratory angular distribution of H^- suggests that, when the correlation angle θ_{12} between the protons in the center of mass (c.m.) of H_3^+ is zero, the internal energy of the $(H_3^+)^*$ is 6.7 eV above the dissociation limit of $H^+ + H^+ + H^-$. No experimental studies to this data have been performed to determine the correlation angle θ_{12} between the two protons. On the other hand, both Klar[3] and Feagin[4] predict that $\theta_{12} = 180°$.

It is obvious that measurements of the angular correlations of the three particles would provide the ultimate tests for the generalized full quantal description of the three-particle systems interacting through the Coulomb interaction. The purpose of this article is to further elucidate the excited states of H_3^+ involved in its dissociation into $H^+ + H^+ + H^-$ before attempting an experiment to determine the momenta of all three dissociation products in coincidence. In the following sections, we will describe the experimental methods used and discuss the new information gained.

II. EXPERIMENTAL METHODS AND RESULTS

The specific experiment we have performed consists of the measurement of the energy distribution of H^- ions produced after the collision of low-keV H_3^+ ions with the

He target and scattered to laboratory angles of 0° and ±0.17°. Although a more complete and detailed description of the apparatus will be reported in a forthcoming article, the salient features of the experiment are briefly described below and the experimental setup is presented in Fig. 1. The incident beam of H_3^+ is produced in a duoplasmatron source that is run at an estimated pressure of 0.3–0.5 Torr. Experiments by Leventhal and Friedman[6] and also by Peart and Dolder[7] indicate that at these operational pressures the majority of the H_3^+ ions leaves the source in the vibrational ground state, a symmetric "breathing" mode. Results of our previously reported experiment on H_3^+ dissociation[8] are also consistent with the H_3^+ being mostly in its lowest vibrational state. The produced ions are extracted from the source, accelerated by an applied potential, focused by einzel lenses, and momentum selected by an analyzing magnet. After the magnet, additional focusing is provided by two pairs of vertical and two pairs of horizontal parallel plates. After passing through a pair of collimation apertures, the H_3^+ beam enters a collision cell, 1.5875 cm (0.625 in.) in diameter and 5.08 cm (2 in.) in height, where it collides with the target gas He. The static gas cell is differentially pumped from the rest of the system, and to minimize the H^- losses via collisions with the background gas, the entire trajectory of H^- after the static cell is kept at a base pressure of 5×10^{-7} Torr. The measurements are done under single-collision conditions which were determined from the linearity of the $L\alpha$-photon counts using a solar-blind photomultiplier also shown in Fig. 1.

Due to the velocity of the c.m. of the H_3^+ molecule, the produced fragments travel in the forward direction and are energy analyzed by a large parallel-plate energy analyzer. The energy-analyzed H^- ions are detected by a pair of microchannel plates (MCP's) in chevron configuration. The electrons produced by the MCP's are collected on individual Cu anodes of 0.060 in. in diameter. The anodes are mounted in a (3×3) square configuration with an interanode spacing of 0.156 in. This setup allows us to measure 0° and ±0.17° laboratory scattering angles at three different energies simultaneously. Because of the finite size of the beam and the anodes, the precision in determining the 0° is estimated to be ±0.03°.

The signal from each anode is connected to an individual preamplifier of Lecroy 7791 board mounted in a shielded box at the vacuum chamber flange. The emitter coupled logic (ECL) output of the preamplifiers is transformed by an ECL-NIM converter (Lecroy Model 4616) and counted by a CAMAC scaler (Lecroy Model 2551) (NIM and CAMAC denote nuclear instrument modulus and computer automated measurement and control, respectively). The scalers are read by the CAMAC-based Lecroy 3500 data acquisition system and stored directly in its histogramming memory. The Lecroy 3500 system also controls the experiment, including all timing and high-voltage settings, which were separately calibrated. A block diagram of the electronics is shown in Fig. 2.

The full width at half maximum resolution of the energy analyzer is determined to be 0.27%. The energy analyzer is calibrated using the following procedure. The central peak in the energy distribution of protons (refer to Fig. 3) produced from the dissociation of H_2^+ colliding with a He target, is determined for a variety of incoming beam energies. This peak occurs at a voltage V on the analyzer and satisfies the relation $(E_0-Q)/2 = k(V)e$, where E_0 is the incoming beam energy in eV, Q the inelastic energy loss in eV, e the electronic charge, and k the dimensionless energy analyzer constant. The value of Q was not previously well known and had to be eliminated from the equations by pairing different measurements, taken at different beam energies. With this pairing procedure, one obtains the relation $\Delta E/2 = k(\Delta V)e$ from which k is determined by linear regression. Therefore, the energy analyzer constants, defined as $k_i = E/eV_i$, where E is the energy (in eV) of the particle and V_i is the required voltage (in volts) to count it on the ith anode pin, are measured directly. The results of these measurements are within 1% of the values obtained using the well-known relation for a parallel-plate analyzer $k_i = R_i/2d$, where R_i is the range of the ith row of pins and d, the distance between the parallel plates. In addition to the above-described calibration procedure, the energy distribution of protons produced by the collision-induced dissociation of 9.987-keV H_2^+ on He is measured. The results of this measurement, shown in Fig. 3, after normalization at an arbitrary

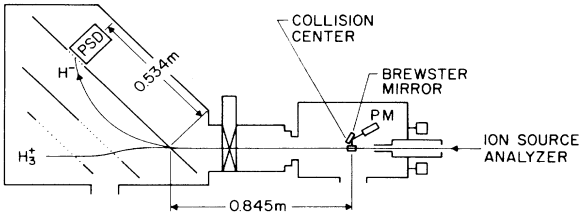

FIG. 1. Schematic experimental arrangement. PSD denotes the multipin position-sensitive microchannel plate detector. PM is a solar-blind photomultiplier used to simultaneously monitor the $L\alpha$-photon counts.

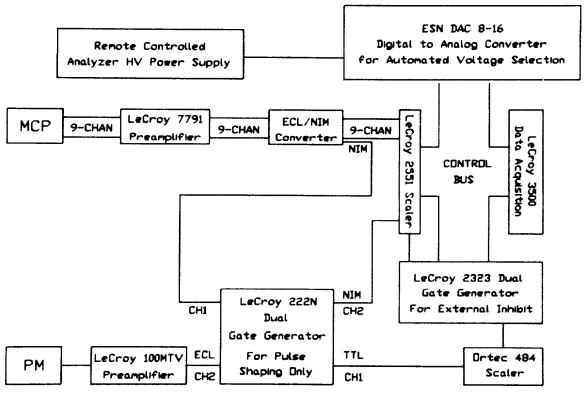

FIG. 2. Block diagram of the electronical setup.

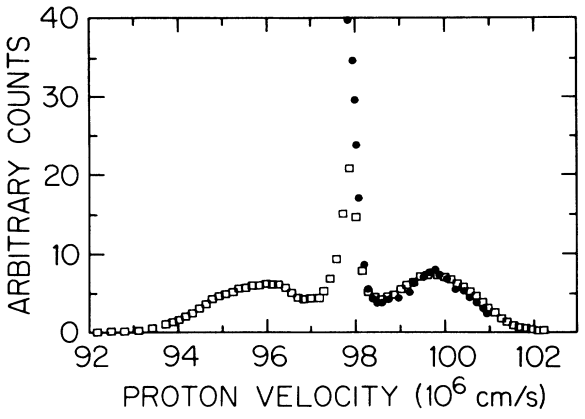

FIG. 3. Laboratory velocity distribution of protons from the collision-induced dissociation of H_2^+ from a He target at 10 keV. Open squares show the present data; solid circles are from Ref. 9 (Gibson and Los, 1967). The two data sets are normalized at an arbitrary point near the forward Aston band.

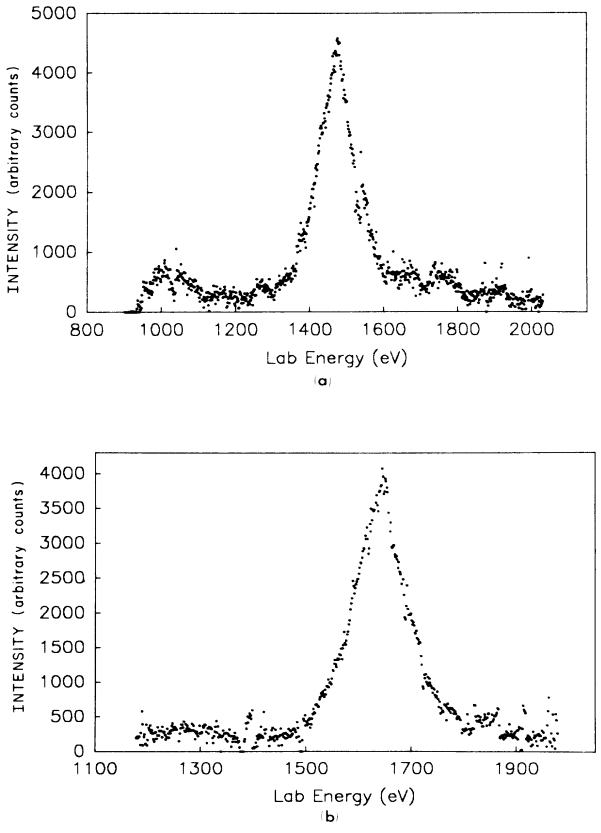

FIG. 4. Laboratory energy distribution of H^- for (a) 4.5 keV and (b) 5.0 keV incoming H_3^+ colliding with a He target. Several spectra were taken at incoming H_3^+ energies ranging from 2.417 keV to 7.0 keV, but no significant change was observed.

point near the Aston band wings, compare very favorably with earlier measurements by Gibson and Los.[9] The discrepancy in the relative heights of the main peak to forward Aston band is due to the fact that MCP's in chevron configuration with a total gain of 10^7 saturate at high counting rates (~ 1 MHz/cm^2).[10] We have also performed an additional independent check of the saturation characteristics of our MCP's to verify the relative ratios of the main peak to the forward Aston band. The ratio of 5.2 we obtain after correcting for the saturation of the MCP's, compares well with the ratio of 5 obtained by Gibson and Los.

A step size of approximately 1.5 eV and data accumulation times ranging from 20 sec to 2.5 min per analyzer voltage are used to obtain spectra in 5–33 h. In a typical raw spectrum, H^- peaks are superimposed on top of a background which is due to secondary electrons accelerated towards the MCP's by the energy analyzer's electrostatic field. This background is not due to induced noise, since it completely disappears from the energy distribution spectra of positive particles. Figures 4(a) and 4(b) show two typical spectra, at 4.5 and 5.0 keV incoming beam energies, respectively. For each spectrum, we have subtracted a straight line obtained by a least-squares fit to the background. Several spectra are taken at 2.417, 3.22, 4.0, 4.5, 4.83, 5.0, 5.5, 6.0, and 7.0 keV of incoming H_3^+ energies, but no significant changes are observed in the form of the distribution.

III. DISCUSSION

In order to collisionally dissociate a molecular projectile through a dissociative electronic state, one has to excite it by an energy amount Q which is provided by the kinetic energy of the projectile. Actually, for a molecule, this inelastic energy loss Q is not a single number but a distribution, since the transition may happen at different internuclear separations of the molecule. The excited molecule, upon dissociation, will have an excess kinetic energy ε. Again, ε is not a single number but a distribution depending on the internuclear distance at which the electronic excitation occurred. For the two-body dissociation, the energy-momentum conservation laws determine uniquely the sharing of this excess kinetic energy by the fragments. For the three-body dissociation, the energy-momentum conservation is not sufficient to determine all the kinematics of the process. Nevertheless, it is still possible to gain insight from the measured energy distribution of a fragment.

The Newton diagram of an excited H_3^+ dissociating into $H^+ + H^+ + H^-$ is shown in Fig. 5. For scattering at 0° in the laboratory, the velocity of the H^- in the c.m. of H_3^+ can be either added to or subtracted from the laboratory velocity of H_3^+ to give a fast or slow component. Thus, in an ideal case where there is a single Q, these two components will give rise to two very sharp H^- peaks in the laboratory frame. These δ-function–type peaks are simulated in Fig. 6 as rectangular boxes to illustrate the concept. In the case of H^- production from the three-body dissociation of H_3^+, the laboratory energy of H^- is related to the incoming beam energy E_0, to the inelastic

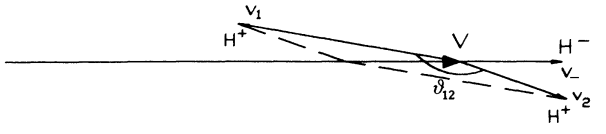

FIG. 5. Newton diagram of the dissociation of the H_3^+ into $H^+ + H^+ + H^-$. V is the velocity of the center of mass (c.m.) of H_3^+ right after the collision, and v_- the velocity of the H^- in the center of mass of H_3^+. v_1 and v_2 are the c.m. velocities of the protons. θ_{12} is the correlation angle between the two protons.

energy loss Q, and to the projectile frame energy of H^- through the vector addition relation

$$E_{\text{lab}} = \tfrac{1}{2} m (V \pm v_-)^2 , \quad (1)$$

$$E_{\text{lab}} = (E_0 - Q)/3 + \varepsilon_- \pm 2[(E_0 - Q)\varepsilon_-/3]^{1/2} , \quad (2)$$

where m is the mass of the proton, V the velocity of the c.m. of H_3^+ right after the collision, and v_- the velocity of the H^- in the c.m. of H_3^+. As one can see from the above equations and Fig. 6, in the laboratory frame, these sharp H^- peaks are separated by an energy equal to $4[\varepsilon_-(E_0 - Q)/3]^{1/2}$. For a given electronic excitation leading to the formation of a fragment, the contribution from a very large number of Q's will produce a pair of broad distributions made of the superposition of these sharp peaks. The centroid of these broad peaks will occur at $(E_0 - Q_0)/3 + \varepsilon_-$ where E_0 is the incoming

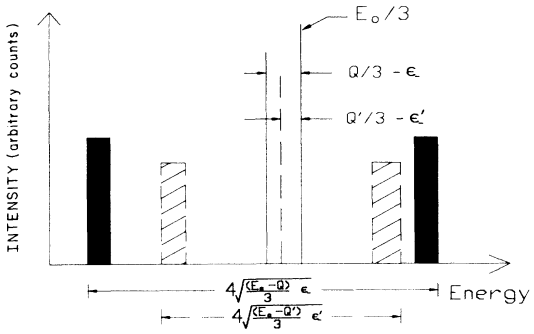

FIG. 6. An idealized laboratory energy distribution of H^- at 0° laboratory scattering angle, where it is assumed that the parent H_3^+ molecule of incoming energy E_0 is excited only at two different internuclear separations with subsequent dissociation. For each excitation, the counts due to the fast and the slow H^- ions are shown by rectangular bins that are drawn to simulate δ functions. The centroid of each pair of bins is shifted from $E_0/3$ by an excitation energy of $(Q/3 - \varepsilon_-)$ and $(Q'/3 - \varepsilon'_-)$, respectively. The energy difference between the fast and the slow H^- components, i.e., the laboratory energy separation between each pair of bins, is $4[\varepsilon_-(E_0 - Q)/3]^{1/2}$ and $4[\varepsilon'_-(E_0 - Q')/3]^{1/2}$, respectively. An actual laboratory energy spectrum would be the superposition of a large number of bins similar to the two pairs shown in this figure.

beam energy and Q_0 an average inelastic energy loss to produce the excited H_3^+ state producing the H^-. If, before the collision, the H_3^+ is in its vibrational ground state, the average inelastic loss is also the most probable inelastic energy loss. In real cases, one has a distribution of vibrational levels and the same fragment may even be produced by different electronic excitations. In some instances, the broad peaks originating from different electronic excitations may overlap considerably, making their identification extremely difficult. The proton energy distribution of Fig. 3 is a good example of such a spectrum. The broad Aston bands on either sides of the main peak are due to the superposition of many different peaks produced by several different mechanisms. Since individual peaks composing the Aston bands may have different centroids, the Aston bands need not be symmetric with respect to the main peak, as in Fig. 3.

As one can see from Fig. 4, the H^- laboratory-frame energy spectrum is made of a single peak with additional smaller features on either sides of the main peak. This paper will concentrate on the mechanisms producing the main peak. The origins of other structures are still under investigation. The main peak is slightly shifted from $E_0/3$ by the same approximate amount for any incoming beam energy. The fact that there is only a single peak is an indication that ε_- values are small. One should note here that, because of the finite aperture size, H^- ions having near-zero projectile frame energies are collected and counted more efficiently in the laboratory frame. The peak of the laboratory distribution corresponds to H^- ions having projectile-frame energies $\varepsilon_- \approx 0$. From Eq. (2), one can see that the laboratory energy for H^- ions having $\varepsilon_- \approx 0$ is $(E_0 - Q)/3$. Therefore, the shift in energy of the maximum of the main peak from $E_0/3$ is a direct measure of an approximate inelastic energy loss of H_3^+ ions that produce H^- ions having near zero kinetic energies in the projectile frame. To estimate the position of their maximum, the laboratory energy distribution peaks are smoothed using the "histogram smoothing" subroutines of the Lecroy 3500 system. Using the energy peak's shift from $E_0/3$, we found that $Q = 60 \pm 12$ eV for H^- ions having near zero kinetic energies in the projectile frame.

Figure 7 shows the approximate limiting energies of the different states that might be involved in the production of H^-. Figure 8 shows the ground and first excited states of H_3^+, the energies of repulsive $H_3^{2+} + e^-$ and $H_3^{3+} + 2e^-$ states in D_{3h} symmetry. In these graphs, molecular energies are determined at the equilibrium separation of the H_3^+ ground state. For the singly excited $(H_3^+)^*$ states we have used the energy curves as calculated by Schaad and Hicks.[11] The ground state of H_3 is obtained from a calculation by Kulander and Guest.[12] The excited states of H_3 are estimated from the molecular-orbital (MO) calculations by Jungen,[13] and also by Martin,[14] which are in good agreement with the observed spectral lines.[15–18] The energy of $H_3^{2+} + e^-$ state in D_{3h} symmetry is obtained from the repulsive ground-state energy surface of H_3^{2+} as calculated by Conroy.[19] We have used the atomic energy tables by Moore[20] for the He en-

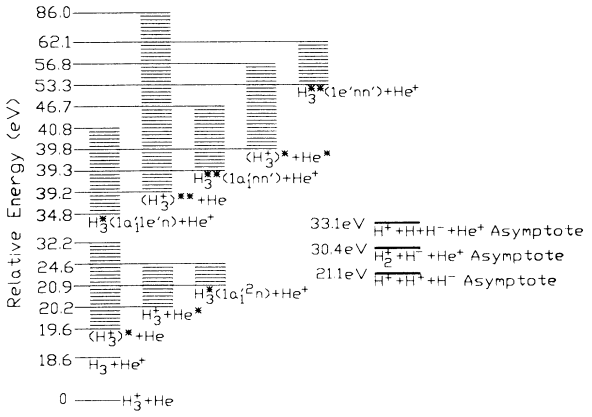

FIG. 7. Approximate limiting energies of states relative to the $H_3^+ + He$ ground state that might be involved in the production of H^-. The energies of H_3^+ and H_3 are taken at the equilibrium separation of H_3^+. Asymptotic values of H^--producing channels are also marked.

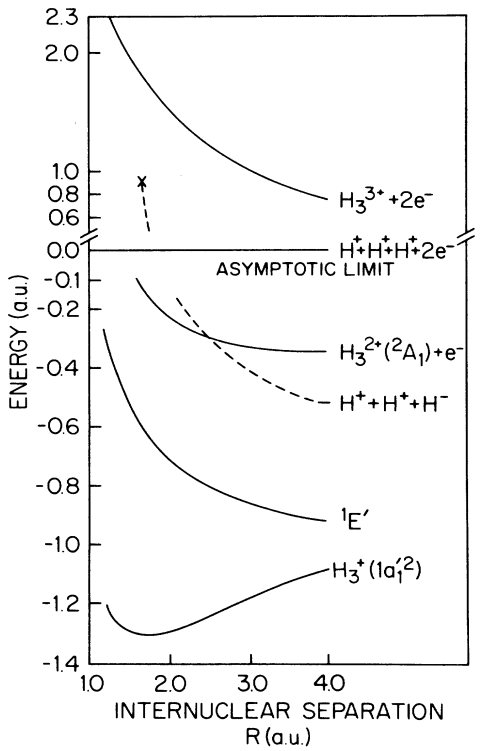

FIG. 8. The ground and first excited states of H_3^+ and the energies of repulsive $H_3^{2+}+e^-$ and $H_3^{3+}+2e^-$ states in D_{3h} symmetry. Note that different scales are used at the top and the bottom of the figure. The cross corresponds to the measured inelastic energy loss of 60 eV. The dashed line is drawn to guide the eye to the $H^+ + H^+ + H^-$ asymptotic level.

ergy levels.

It should be noted that the energy limits of most of the states shown in Fig. 7 do not account for the experimentally measured inelastic energy loss $Q = 60 \pm 12$ eV. These states, then, are not the ones that produce the H^- main peak in our laboratory energy spectra. All three of the possible states that may produce H^-, i.e., $(H_3^+)^{**}+He$, $(H_3^+)^*+He^*$, and $H_3^{**}(1e'nn')+He^+$, require two-electron processes for their excitation. The transition from the $H_3^+ + He$ to the $H_3^{**}(1e'nn')+He^+$ state involves a charge transfer to an excited molecular orbital with simultaneous excitation of both electrons of the $1a_1'$ ground-state MO. This charge transfer process would be less likely than a two-electron excitation of H_3^+, since there is a large energy defect (of the order of 20 eV) between the He($1s$) orbital and the excited MO's of H_3. Either of the two remaining processes produces an excited H_3^+ which then dissociates into $H^+ + H^+ + H^-$. Presently, the details of the excitation mechanism are unknown.

An approximate projectile-frame energy distribution can also be extracted from the laboratory energy spectrum of H^-. We assumed an isotropic projectile frame H^- distribution as did existing deconvolution methods in the literature.[21–23] The thickness of the H_3^+ beam was approximately one-half of the anode diameter. We neglected the effects due to the thickness of the beam or to its angular divergence. The method is based on the principle that the number of H^- ions reaching the detector is independent of the reference system in which this number is expressed. Assuming an isotropic distribution, in the c.m. of H_3^+, the number of ions reaching the detector's aperture is proportional to the subtended solid angle whose central half-angle in the projectile frame is related to the central half-angle in the laboratory frame through the usual Galilean velocity transformation. This procedure leads in a natural way to the well-known Jacobian of the Galilean velocity transformation. Only the main peak of the laboratory distribution in the vicinity of $E_0/3$ is transformed to the c.m. of the dissociating molecule. Since $E_0 \gg Q(R)$, we have assumed a single Q, the value which corresponds to the maximum of the peak, for the transformation of the main peak. The approximate projectile-frame energy distribution, obtained from the transformation of the laboratory spectra at 5.0, 5.5, 6.0, and 7.0 keV incoming beam energies, is presented in Fig. 9. From this graph, the most probable projectile-frame energy of H^- is estimated to be approximately 0.75 eV.

The expressions given in Fig. 6 allow us to determine the maximum H^- projectile-frame energy by estimating the base width of the main peak of the laboratory H^- energy spectra similar to the ones presented in Fig. 4. From a total of 33 spectra taken at different incoming beam energies, we determined the maximum H^- projectile-frame energy $(\varepsilon_-)_{max} = 2.31 \pm 0.2$ eV, which is consistent with the projectile-frame H^- energy distribution of Fig. 9. This value and the total excess kinetic energy of the fragments in the c.m. of dissociating H_3^+, obtained from Fig. 8, coupled with the energy-momentum conservation, establish limits on the correlation angle θ_{12}.

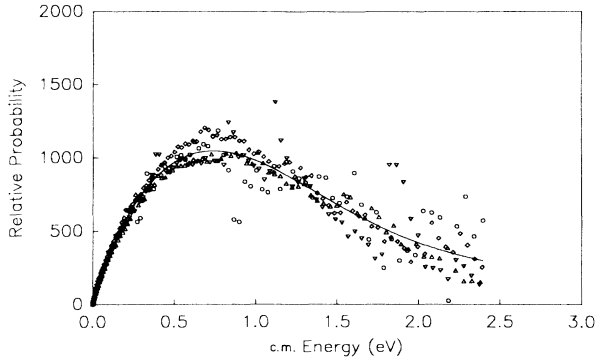

FIG. 9. Approximate projectile-frame energy distribution of H^- fragments forming the central peak of the laboratory spectrum. Circles are for 5.0 keV, triangles for 5.5 keV, inverted triangles for 6.0 keV, and diamonds for 7.0 keV incoming H_3^+ energies. The solid line is a least-squares polynomial fit to the data. Note that the most probable H^- energy in the projectile frame is approximately 0.75 eV.

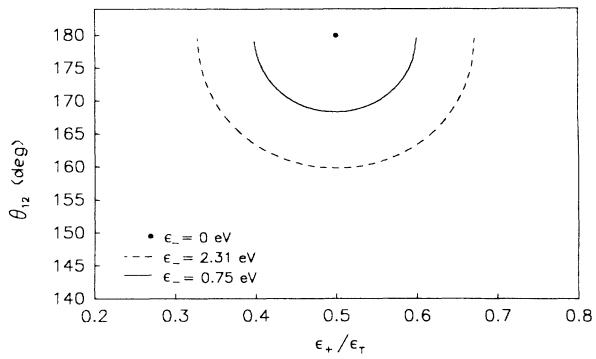

FIG. 10. For $H_3^+ \rightarrow H^+ + H^+ + H^-$, the distribution of the correlation angle θ_{12} between the two protons, as a function of the energy-sharing ratio of the protons. ϵ_+ is the energy of one of the protons: ϵ_t is the available energy to be shared by the two protons. The solid curve is for the most probable H^- projectile-frame energy, the dashed line for the maximum projectile-frame energy of H^-, and the single point for the minimum energy of H^- in the projectile frame, where we assume no He excitation during the collision. If He is excited during the collision, the minimum θ_{12} for the most probable projectile-frame energy of H^- becomes 163°.

One should note here that in the case of the three-body dissociation, the additional degree of freedom due to the sharing of the extra kinetic energy by the two protons, does not give a unique θ_{12}, but a distribution depending upon how the excess kinetic energy is shared between the protons. In the classical Wannier theory of the threshold electron impact ionization, all energy-sharing configurations equally probable.[24] Therefore, there is no reason *a priori* to prefer one configuration over another. Nevertheless, the correlation angle is still limited to values near 180°. The θ_{12} distribution as a function of the ratio of the energy of one of the protons to the total c.m. kinetic energy available for the two protons is presented in Fig. 10 for the case where He is not excited. For the most probable H^- energy in the c.m., we find that the correlation angle is larger than approximately 170°, depending on the energy sharing. In the case of simultaneous H_3^+ and He excitations, the shape of this distribution does not change appreciably, but the minimum θ_{12} angle, for the most probable H^- energy in the c.m., is limited to 163°. One should note that in the case of H_3^+ dissociating into $H^+ + H^+ + H^-$, there are energy sharing configurations forbidden by the energy-momentum conservation. These forbidden regions are a function of the energy of the H^-.

IV. CONCLUSIONS

We have measured the laboratory energy distribution of H^- produced from H_3^+ colliding with He targets at low-keV energies and determined its approximate projectile-frame energy distribution. We found an inelastic energy loss of 60±12 eV for H^- ions having near zero kinetic energies in the c.m. of the dissociating H_3^+, which established that the H^- ions with near zero kinetic energies in the projectile frame are produced by a two-electron process. Our measurements suggest that the most plausible mechanism for H^- production with near zero projectile-frame energies is the electronic excitation of H_3^+ with subsequent dissociation into $H^+ + H^+ + H^-$. In this case, it is possible to limit the correlation angle θ_{12} between the protons. For the most probable projectile-frame energy of the H^-, the correlation angle is limited to values larger than 170°, if He is not excited. The possibility of He being excited does not change any part of our interpretation, except for slightly lowering the limit on the correlation angle between the protons for the maximum projectile-frame energy of H^- to values larger than 163°. In either case, we are in reasonably good agreement with the predictions of the Wannier theory applied to three-particle systems of arbitrary mass,[2,3] where the correlation angle between the protons, in the c.m. of dissociating H_3^+, is calculated to be 180°.

ACKNOWLEDGMENT

The support of this work by the National Science Foundation through a grant is gratefully acknowledged.

[1]F. H. Read, in *Electron Impact Ionization*, edited by T. D. Mark and G. H. Dunn (Springer-Verlag, New York, 1985), p. 42 (and references therein).

[2]H. Klar Z. Phys. A **307**, 75 (1982).

[3]J. M. Feagin, J. Phys. B **17**, 2433 (1984).

[4]D. L. Montgomery and D. H. Jaecks, Phys. Rev. Lett. **51**, 1862 (1983).

[5]I. Alvarez, C. Cisneros, J. de Urquaijo, and T. J. Morgan, Phys.

Rev. Lett. **53**, 740 (1984).
[6]J. Leventhal and L. Friedman, J. Chem. Phys. **50**, 2928 (1969).
[7]B. Peart and K. T. Dolder, J. Phys. B **7**, 1567 (1974).
[8]O. Yenen and D. H. Jaecks, Phys. Rev. A. **32**, 836 (1985).
[9]D. K. Gibson and J. Los, Physica **35**, 258 (1967).
[10]M. I. Green, P. F. Kenealy, and G. B. Beard, Nucl. Instrum. Methods **126**, 175 (1975).
[11]L. J. Schaad and W. V. Hicks, J. Chem. Phys. **61**, 1934 (1974).
[12]K. C. Kulander and M. F. Guest, J. Phys. B **12**, L501 (1979); see Ref. 8 for the procedure.
[13]M. Jungen, J. Chem. Phys. **71**, 3540 (1979).
[14]R. L. Martin, J. Chem. Phys. **71**, 3541 (1979).
[15]G. Herzberg, J. Chem. Phys. **70**, 4806 (1979).
[16]I. Dabrowski and G. Herzberg, Can. J. Phys. **58**, 1238 (1980).
[17]G. Herzberg and J. K. G. Watson, Can. J. Phys. **58**, 1250 (1980).
[18]G. Herzberg, H. Lew, J. J. Sloan, and J. K. G. Watson, Can. J. Phys. **59**, 428 (1981).
[19]H. Conroy, J. Chem. Phys. **51**, 3979 (1969).
[20]C. E. Moore, *Atomic Energy Levels*, Natl. Bur. Stand. (U.S.) Circ. No. 467 (U.S. GPO, Washington, D.C., 1958).
[21]S. J. Anderson, J. Chem. Phys. **60**, 3278 (1974).
[22]S. C. Goh, Aust. J. Phys. **34**, 43 (1981).
[23]J. Los and T. R. Govers, in *Collision Spectroscopy*, edited by R. G. Cooks (Plenum, New York, 1978), p. 317.
[24]S. Cvejanovic and F. H. Read, J. Phys. B **7**, 1841 (1974).